JOURNAL OF
Materials
CHEMISTRY

Confinement of a polaronic state in poly(*m*-phenyleneoligothienylene)

Tadatake Sato, Kiyotaka Hori and Kazuyoshi Tanaka*

Department of Molecular Engineering, Graduate School of Engineering, Kyoto University, Sakyo-ku, Kyoto 606-01, Japan

In order to build polaronic ferromagnetic polymers, poly(*m*-phenylenequaterthienylene) (P*m*PhTh$_4$) was designed and successfully prepared by electrochemical polymerization of 1,3-bis(2,2′-bithiophen-5-yl)benzene. The electronic properties of neutral and doped P*m*PhTh$_4$ were investigated by both experimental and theoretical methods. It was confirmed that the polaronic spins generated by the doping were confined to the neighbourhood of the quaterthienylene unit. For comparison, the electronic properties of the previously reported P*m*PhTh$_2$ were also examined.

The molecular design and synthesis of organic ferromagnets has been one of the most fascinating subjects in recent years, since Mataga reported an organic polymeric ferromagnet based on a topological array of carbenes accommodating unpaired electrons ferromagnetically correlating throughout the polymer skeleton.[1] The polaronic ferromagnet proposed by Fukutome *et al.*[2] is one of the more realistic strategies to create ferromagnetic conjugated polymers consisting of two alternating blocks—spin supplier block (SSB) and ferromagnetic coupling block (FCB). Along these lines, a polymer with high spin order ($S=5/2$ at maximum where S is the total spin quantum number) has been prepared using the octatetraene unit as the SSB.[3]

Conjugated polymers consisting of heteroaromatic rings, such as polythiophene, have attracted much attention. High electrical conductivity is generally observed in their oxidised states.[4] These phenomena have been explained by the formation of a polaron and/or bipolaron induced in the polymer chain by doping. From the viewpoint of designing the SSB described above, a polaron can be utilised as a spin centre in a polaronic ferromagnet. There are two important conditions to be met in this scenario: (*i*) the stable polarons must be confined within the SSB and (*ii*) bipolarons should not form because they cancel out the electron spins.

Recently, various oligothiophenes have been studied as model compounds for polythiophene.[5–7] Generally, the cationic state of oligothiophenes with shorter conjugation length is highly reactive and couples immediately and irreversibly. However, it has been reported that a stable cationic state was observed in quaterthiophene[5] of almost the same size as the spatial extent of the polaron theoretically predicted.[8] Moreover, this size is almost half the theoretically predicted spatial extent of the bipolaron[8] and, hence, makes the bipolaronic state unstable.

The block copolymer consisting of *m*-phenylene and bithienylene has already been synthesised by electrochemical polymerization as the material for electrochromic devices.[9] A preliminary study on polaronic ferromagnetic polymers by employing thienylene and bithienylene as SSB has reported that the polymer containing bithienylene unit showed $S>1/2$ upon I_2 doping.[10] In the present study, we have attempted to characterise the electronic properties of poly(*m*-phenylenequaterthienylene) (P*m*PhTh$_4$) synthesised for the first time. This is a block copolymer consisting of the quaterthienylene unit as the SSB and the *m*-phenylene unit as the FCB, which can be prepared by electrochemical polymerization. Hence P*m*PhTh$_4$ is expected to have the maximum spatial extent of the polaron in the SSB as described above. The magnetic properties of electrochemically doped P*m*PhTh$_2$ and P*m*PhTh$_4$ were examined in detail by *in situ* electron paramagnetic resonance (EPR) measurements for comparison of these two polymers. Moreover, crystal orbital (CO) calculations of these polymers in both the neutral and the oxidised states were also carried out for analysis of their electronic structures.

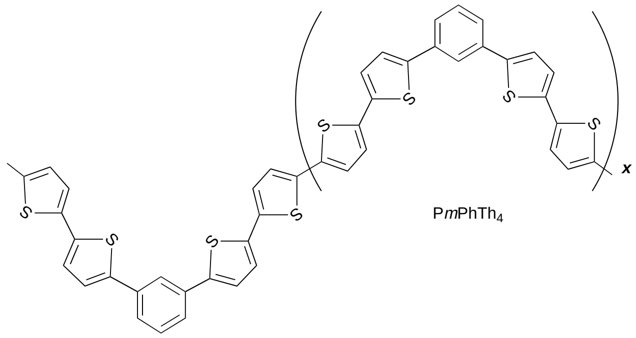

P*m*PhTh$_4$

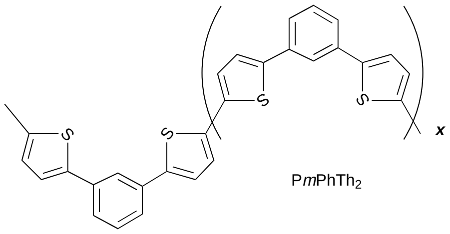

P*m*PhTh$_2$

Experimental

Chemicals

1,3-Di(2-thienyl)benzene (*m*PhTh$_2$) and 1,3-bis(2,2′-bithiophen-5-yl)benzene (*m*PhBT$_2$) were synthesised and then applied to the electrochemical polymerization as the starting monomers. Details of the synthetic procedures are to be reported elsewhere.[11] CH_2Cl_2 used for *in situ* EPR measurement was distilled over CaH_2 and stored under N_2. $Bu^n{}_4NBF_4$, CH_2Cl_2 and acetonitrile used for electrochemical polymerization and other measurements were of the best commercial grade available and used without further purification.

Electrochemical polymerization

Poly(*m*-phenyleneoligothienylene) (P*m*PhTh$_n$: $n=2,4$) films were prepared on an indium–tin oxide (ITO) glass electrode by electrochemical polymerization. The electrochemical polymerization was carried out in CH_2Cl_2 solution containing $Bu^n{}_4NBF_4$ (100 mM) and the starting monomer: *m*PhBT$_2$ (1 mM) or *m*PhTh$_2$ (5 mM). A Pt plate and a saturated calomel electrode (SCE) were used as the counter and the reference electrodes, respectively. The polymerization of mPhBT$_2$ or mPhTh$_2$ was carried out under constant polymerization potential at 1.18 or 1.35 V *vs.* SCE, respectively. Thickness of the film was controlled by the amount of charge supplied during the polymerization.

Prior to the successive measurements the film obtained was electrochemically reduced at −0.5 to 0 V *vs.* SCE until the reduction current fell below 1.0 μA. For the *in situ* optical and EPR measurements, the neutral films thus obtained were doped again in the electrolyte solution containing $Bu^n{}_4NBF_4$ (100 mM). The dopant concentration *y* (per monomer unit) was controlled by the applied potential (V *vs.* SCE) and conventionally evaluated from the amount of charge released during the electrochemical reduction and the mass of the reduced polymers.

Miscellaneous measurements

The structure of the polymers was confirmed by the Fourier transform infrared (FT-IR) spectra measured with a BIO-RAD FTS-30 FT-IR spectrometer. The measurements of the present PmPhTh$_n$ films were carried out using the attenuated total reflection (ATR) method without removing them from the ITO glass. The cyclic voltammogram (CV) measurements on PmPhTh$_4$ were performed at room temperature. PmPhTh$_4$ film was prepared on a Pt wire and then used in CV measurements in the electrolyte solution: CH_3CN containing $Bu^n{}_4NBF_4$ (100 mM). A Pt plate and the SCE were used as the counter and the reference electrodes, respectively. The *in situ* optical absorption measurements were performed with a Shimadzu UV365 spectrophotometer. PmPhTh$_4$ films were prepared on ITO glass and assembled in a 1 cm quartz cell. The measurements were carried out by applying appropriate potentials in the same electrolyte solution as that for the CV measurements.

The *in situ* EPR measurements were performed with a JEOL RE-2X spectrometer at the X band (9.1 GHz) at room temperature. For these measurements, a special electrochemical cell was made in a 5 mm diameter quartz tube. This cell contained a Pt plate (0.3×0.8 cm^2) as the working electrode on which a PmPhTh$_n$ film (*ca.* 2–3 μm thickness) had been prepared. It also contained Pt and Ag wires as the counter and the reference electrodes, respectively,[12,13] for the electrochemical doping in the EPR cavity. The EPR measurements were carried out after the anodic current for the doping reached quasi-equilibrium by applying appropriate potentials. An Mn^{2+}–MgO solid solution was used for the determination of the peak-to-peak linewidth (ΔH_{pp}) and the *g* value, and a $CuSO_4 \cdot 5H_2O$ crystal as the reference for the calculation of the spin concentration.

Method of calculation

The electronic-structure calculations were performed on the basis of the one-dimensional tight-binding self-consistent field (SCF) CO method under the CNDO/2 approximation including all the valence electrons.[14] The restricted Hartree–Fock (RHF) and the unrestricted (UHF) methods were used for the calculations of the neutral and the ferromagnetic oxidised states, respectively.

The program employed for the present calculations is able to handle the screw-axis symmetry as well as the translational symmetry. Note that the screw-axis symmtery is defined by the combination of the pitch and the rotation angle. The portion of the structures shown in parentheses were used as the unit cell. In the present study, the polymer structure was constructed by translating the unit cell with rotation by 180° around the translational axis at the same time. The initial geometries of the present model polymers were assumed to be planar, and then optimised by the energy gradient method[15] in their neutral state. The cationic states of the structure thus optimised were calculated by removing an electron from each unit cell. The number of representative wave vectors was chosen as 21 with a regular interval ($\pi/10a$, where a is the translational length) in the Brillouin zone. The overlap and the electron repulsion integrals were considered as far as the second and the third nearest-neighbouring cells for PmPhTh$_4$ and PmPhTh$_2$, respectively.

Results and Discussion

The structure of PmPhTh$_n$

The FT-IR ATR spectra of PmPhTh$_n$ films are shown in Fig. 1 together with those of the monomers. The bands at 705 cm^{-1} (labelled **A**) assigned to the C—H out-of-plane bending vibration of 2-substituted thiophenes[16] were seen in the spectra of the monomers but almost vanished in those of the polymers. In contrast, the band at about 785 cm^{-1} (labelled **B**) assigned to the C—H out-of-plane bending vibration of 2,5-substituted thiophenes[17] was observed in the spectra of both the mPhBT$_2$ and polymers. From these results, it is evident that mPhTh$_2$ and mPhBT$_2$ coupled at their α-positions as was expected. Moreover, the bands at 690, 790 and 875 cm^{-1} (labelled **C**) were assigned to the C—H out-of-plane bending vibration of *m*-phenylene. Among these, the band at 875 cm^{-1} assigned to the *m*-phenylene was weak in the spectra of the starting monomers. In the FT-IR ATR spectra of polymers, only the intense bands can be observed; the band at 790 cm^{-1} was observed as a shoulder on that for the C—H out-of-plane bending vibration of 2,5-substituted thiophene, and that at 875 cm^{-1} was unclear. Similar IR spectra have been observed for PmPhTh$_2$.[9] It was thus confirmed that PmPhTh$_n$ polymers have the structures shown.

Electrochemistry of PmPhTh$_4$

Two steps of redox processes were observed in the CV results for PmPhTh$_4$ as seen in Fig. 2. These redox processes were reversible for at least 10 cycles. The redox potentials ($E_{1/2}$) corresponding to each step were $E_{1/2}{}^1 = 0.98$ and $E_{1/2}{}^2 = 1.24$ V *vs.* SCE. In oligothiophene and polythiophene, the oxidation peak potentials (E_{pa}) decrease with increasing conjugation

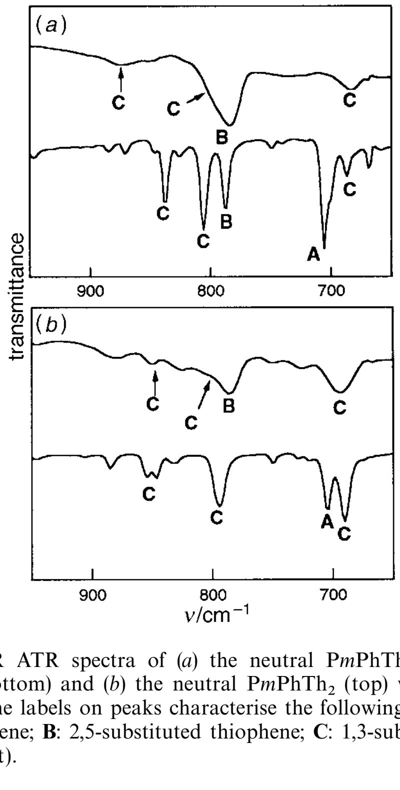

Fig. 1 FT-IR ATR spectra of (*a*) the neutral PmPhTh$_4$ (top) with mPhBT$_2$ (bottom) and (*b*) the neutral PmPhTh$_2$ (top) with mPhTh$_2$ (bottom). The labels on peaks characterise the following: **A**: 2-substituted thiophene; **B**: 2,5-substituted thiophene; **C**: 1,3-substituted benzene (see text).

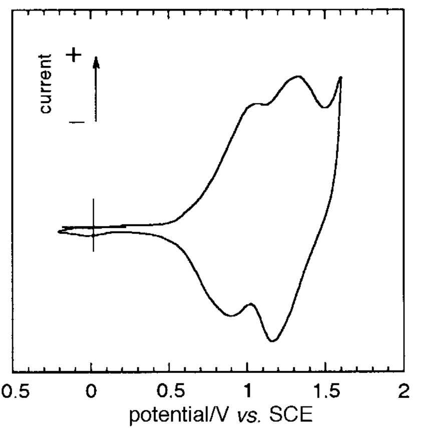

Fig. 2 CV of P*m*PhTh$_4$ in CH$_3$CN solution containing 0.1 M of Bu$^n_4$NBF$_4$. Scan rate: 200 mV s^{-1}.

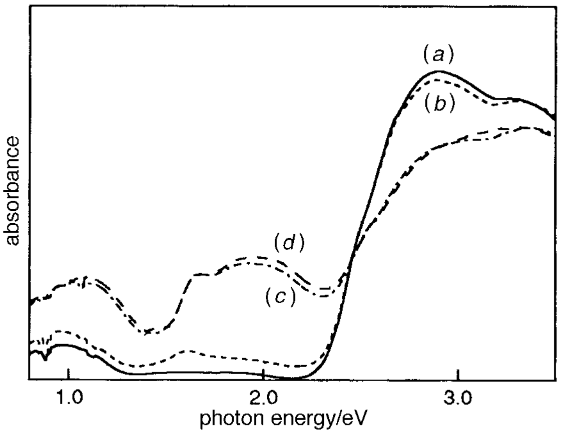

Fig. 3 Optical absorption spectra of P*m*PhTh$_4$ at various dopant concentrations *y*: (*a*) neutral; (*b*) $y=0.010$; (*c*) $y=0.50$; (*d*) $y=1.1$.

length in proportion to the reciprocal of the number of thiophene rings.[18] The oxidation peaks of P*m*PhTh$_4$ were observed at $E_{pa}^{1}=1.06$ V and $E_{pa}^{2}=1.32$ V *vs.* SCE under the present conditions. Note that one oxidation peak was observed at 0.87–1.12 V *vs.* SCE for polythiophene, polybithiophene and polyterthiophene.[19] In contrast, for the quaterthiophene derivative, it has been reported that two oxidation peaks were observed at $E_{pa}^{1}=1.04$ and $E_{pa}^{2}=1.36$ V *vs.* SCE.[18] These results strongly suggest that the oxidised states of P*m*PhTh$_4$ are almost confined in quaterthienylene units. Moreover, the second redox process should be assigned to the formation of the dication in quaterthienylene units.

Incidentally, the electrical conductivity of as-grown P*m*PhTh$_4$ (that is, the doped sample) film measured by the four probe technique was 2.3×10^{-4} S cm^{-1}. This conductivity is similar to that of quaterthiophene derivatives, 3.0×10^{-6}–7.1×10^{-4} S cm^{-1} for cation radical salts of α,α′-dimethyl-substituted quaterthiophene (DMQtT),[20] rather than that of polythiophene, 10–370 S cm^{-1}.[4]

Optical absorption measurements

The colour of the P*m*PhTh$_4$ film changed from deep yellow (pristine) to dark blue (doped) with doping. The *in situ* optical absorption spectra at various dopant concentrations *y* are shown in Fig. 3. The peak at 2.88 eV (430 nm) of the neutral P*m*PhTh$_4$ was assigned to the π–π* transition, which is higher than that of polythiophene observed at 2.56 eV (485 nm).[19] However, the former peak is smaller in comparison with the reported values for quaterthiophene: for the unsubstituted quaterthiophene in CH$_2$Cl$_2$ solution the π–π* transition peak was observed at 3.68 eV (337 nm)[5] and for DMQtT at 3.12 eV(397 nm) in CH$_2$Cl$_2$ solution[6] and at 3.68 eV (337 nm) for vacuum-evaporated film.[7] This result indicates that the π-conjugation of the quaterthienylene unit is somewhat extended due to its connection with *m*-phenylene units. With an increase in the dopant concentration, the π–π* transition peak was suppressed and shifted to the higher energy region with the additional peaks appearing at about 1.0 eV (1240 nm) and 1.9 eV (653 nm). Similar changes have generally been seen in polythiophene and polypyrrole, which have been explained in terms of the formation of polarons.[21] Additional peaks derived from the polaronic state were observed at 0.65 and 1.5 eV for the doped polythiophene,[22] and at about 1.0 and 1.8 eV for the vacuum-deposited DMQtT.[7] Thus, it is also probable that the present additional peaks of P*m*PhTh$_4$ can be attributed to the polaronic state confined in the quaterthiophene unit.

EPR measurements

The properties of spins in P*m*PhTh$_4$ induced by electrochemical doping were examined by EPR measurements. The EPR spectra and data for various dopant concentrations are shown in Fig. 4 and Table 1. For comparison, the results of P*m*PhTh$_2$ at a dopant concentration $y=0.048$ are also shown. The EPR spectra of all the doped samples showed a single line with no hyperfine splitting. In the neutral state, no EPR signal was observed for either P*m*PhTh$_2$ or P*m*PhTh$_4$. This indicates that the spins did not originate from the structural defect generated during the polymerization but were brought about by electrochemical doping.

The EPR lineshapes were narrow with the peak-to-peak linewidths (ΔH_{pp}) in the range of 1.00–1.33 G, being similar to that of polythiophene ($\Delta H_{pp}=1.5$ G for the 10 mol% BF$_4^-$-doped example).[23] Narrow EPR signals observed in doped polythiophene are usually explained by motional narrowing. Moreover, the present values are much smaller than that of the doped DMQtT ($\Delta H_{pp}=2.25$ and 2.20 G for the I$_2$- and the

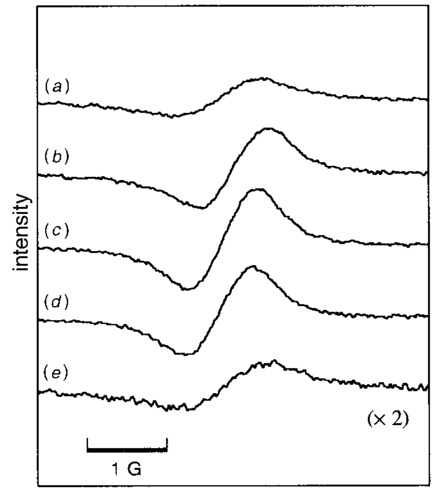

Fig. 4 EPR spectra of P*m*PhTh$_4$ at various dopant concentrations *y*: (*a*) $y=0.73$; (*b*) $y=0.60$; (*c*) $y=0.49$; (*d*) $y=0.29$; (*e*) $y=0.11$.

Table 1 EPR data of P*m*PhTh$_n$ ($n=2,4$) measured at room temperature

polymer	dopant concentration (y)	g value	ΔH_{pp}/G	N_s/spins g^{-1}
P*m*PhTh$_4$	0.73	2.0023	1.17	5.5×10^{19}
	0.60	2.0022	1.08	7.8×10^{19}
	0.49	2.0022	1.00	9.0×10^{19}
	0.29	2.0022	1.04	7.9×10^{19}
	0.11	2.0022	1.33	3.7×10^{19}
P*m*PhTh$_2$	0.048	2.0029	2.39	2.3×10^{18}

$NOPF_6$-doped examples, respectively).[24] The g values of the doped PmPhTh$_4$ were almost constant at 2.0022–2.0023, reminiscent of values for π-radicals delocalised on a carbon skeleton, although the signal intensity changed with y. This g value is similar to those observed for polythiophene (2.0023–2.0026),[23] poly(disilanylenequaterthienylene) (2.0022–2.0026)[24] and DMQtT (2.0021–2.0023).[25]

The EPR lineshapes of PmPhTh$_4$ were close to the Gaussian type since the values of $\Delta H_{1/2}/\Delta H_{pp}$ were in the range of 1.88–2.15 at various y, where $\Delta H_{1/2}$ stands for the half-height linewidth. Note that rigorous Lorentzian and Gaussian lineshapes give $\Delta H_{1/2}/\Delta H_{pp}$ values of 2.40 and 1.92, respectively. This again confirms that the spins in PmPhTh$_4$ are spatially more confined compared with usual π-conjugated polymers such as, for instance, polyacetylene, showing an almost completely Lorentzian lineshape.[26] Furthermore, the notable difference in the ΔH_{pp} value between PmPhTh$_2$ and PmPhTh$_4$ clearly indicates that the spins are more spatially confined in the former.

The EPR signal intensities of the doped PmPhTh$_4$ gradually increased with the dopant concentration ($y = 0.11$–0.49). At similar dopant concentration ($y = 0.50$), additional peaks were observed in the optical absorption spectra as described above. The spin concentrations (N_s) of the doped PmPhTh$_4$ were of the order 10^{19} spins per gram with the maximum value at a dopant concentration of $y = 0.49$, being very similar to those of the doped polythiophene[23] and the doped DMQtT.[25] At this concentration, the doped PmPhTh$_4$ has one spin per 17 quaterthienylene units. This spin concentration is, however, smaller by one order of magnitude than that estimated from the dopant concentration. That is, at this dopant concentration ($y = 0.49$), PmPhTh$_4$ ought to have one polaron per two quaterthienylene units. Moreover, the intensity of the EPR signal considerably decreased with increasing y (*e.g.* 0.60–0.73), although the intensity of the additional optical peaks did not decrease at these dopant concentrations. These results could be interpreted as the generated spins being partially cancelled out by effects, such as interchain antiferromagnetic interactions which become dominant at dopant concentrations $y > 0.49$.

Results of crystal orbital (CO) calculations

The highest occupied (HO) and the lowest unoccupied (LU) CO patterns of the neutral polymers are illustrated in Fig. 5. The HOCO and the LUCO are of π-type. Moreover, the HOCO and the LUCO patterns on oligothienylene units are favourable for the aromatic- and quinoid-like structures, respectively, due to their in-phase overlapping patterns.[27] Note that there occurs a 'cutting' of π-conjugation at the centre of m-phenylene signifying the confinement of π-electron delocalization within the thienylenes plus vinylene part in the m-phenylene moiety. As a result, the HO and the LU bandwidths become narrow as shown in Fig. 6. This agrees well with the experimental optical absorption and EPR measurements described above. The band structures of the oxidised states at $y = 1$ are shown in Fig. 7. The up-spin HO band corresponds to the ferromagnetic band, whose widths (Δ_0) are 0.70 and 0.32 eV for PmPhTh$_2$ and PmPhTh$_4$, respectively. Such narrow bands, particularly that of PmPhTh$_4$, give a physical source for achieving ferromagnetic spin alignment.

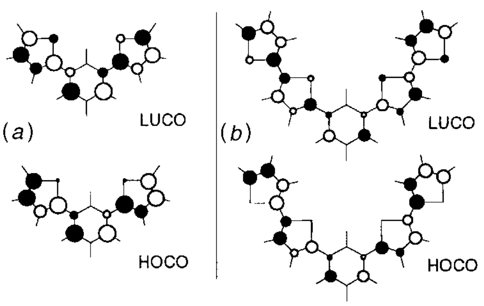

Fig. 5 Patterns of the HOCO and the LUCO of the neutral (*a*) PmPhTh$_2$ and (*b*) PmPhTh$_4$. Note all the atomic orbital lobes are of π-type to the polymer plane.

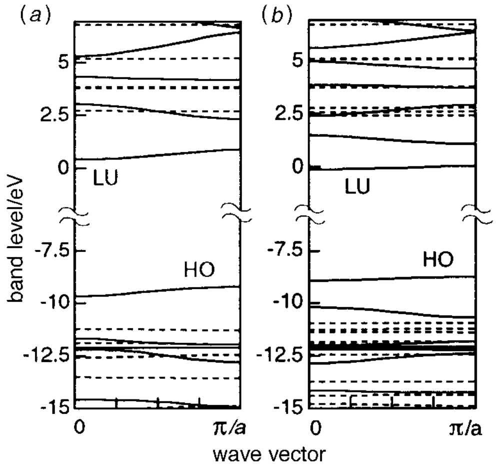

Fig. 6 Band structures of the neutral (*a*) PmPhTh$_2$ and (*b*) PmPhTh$_4$. Solid and broken lines indicate π- and σ-bands, respectively.

In the present oxidised polymers, all the calculated spins were found to be π-type and the spin densities are shown in Fig. 8. Only a small spin density was found on the sulfur atom,

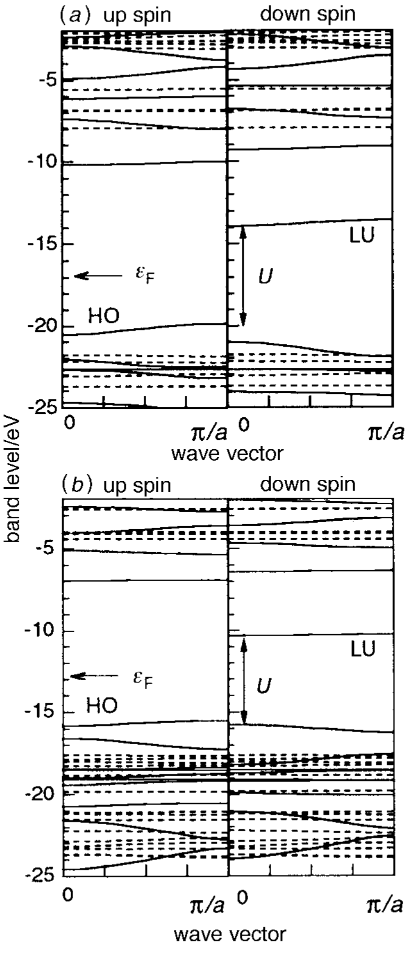

Fig. 7 Band structures of the oxidised (*a*) PmPhTh$_2$ and (*b*) PmPhTh$_4$. Solid and broken lines indicate π- and σ-bands, respectively. U and ε_F stand for the on-site Coulomb energy and the Fermi level, respectively.

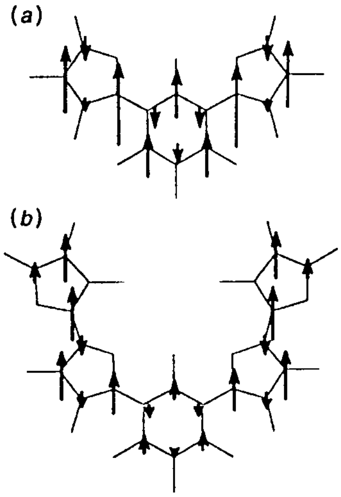

Fig. 8 Spin distribution of the oxidised (*a*) P*m*PhTh$_2$ and (*b*) P*m*PhTh$_4$. Up and down arrows represent the up-spin and down-spin densities, respectively.

which is in agreement with the g value from the EPR measurement. The up-spins are distributed on the carbon atoms not only in the oligothienylene unit but in a part of the *m*-phenylene unit. This indicates that the *m*-phenylene unit works well as an FCB. An irregular alignment of up- and down-spins, in other words spin frustration, is seen in oligothienylene units due to their five-membered ring similarly to that seen by molecular orbital calculations on cationic DMQtT.[25] With the condition that up-spin electrons occupy such a narrow (or localised) HO band as shown above whose level is, say, ε_0 and that ε_0 is well below the Fermi level (ε_F; see Fig. 7), the corresponding down-spin LU level is raised by the amount of on-site Coulomb energy U. It is known that if this LU level lies well above ε_F, the density of down-spin electrons is nearly zero.[28] In particular, under the conditions $-\varepsilon_0 \gg \pi\Delta_0$ and $\varepsilon_0 + U \gg \pi\Delta_0$, the solution of $n\uparrow \approx 1$ and $n\downarrow \approx 0$ can be observed, where $n\uparrow$ and $n\downarrow$ are the number of up- and down-spin electrons at the localised level, respectively. Hence it can be said that the present oxidised P*m*PhTh$_4$ is suitable as a ferromagnetic polymer at least without consideration of interchain antiferromagnetic coupling.

Conclusion

The molecular design of a novel polaronic ferromagnetic polymer and its actual synthesis have been performed with a combination of quaterthienylene and *m*-phenylene units. There are five major findings in the present study.

(1) The novel polymer, P*m*PhTh$_4$, was designed towards building up a polaronic ferromagnetic polymer, in which quaterthienylene and *m*-phenylene were used as the SSB and FCB, respectively.

(2) Polarons were induced in polymer chains by electrochemical doping, which was confirmed by the appearance of an additional optical band in the sub-gap region. The existence of polaronic spins was confirmed by an EPR signal of a narrow Gaussian-type.

(3) Both *in situ* optical and EPR spectra indicated that the generated polaronic spins were confined in the neighbourhood of the quaterthienylene unit. This ensures that the *m*-phenylene unit duly works as an SSB.

(4) From the crystal orbital patterns of the polymer, the confinement of π-electron delocalization within the thienylenes and vinylene part in *m*-phenylene moiety is shown. As a result, the HO and the LU bandwidths become narrow. This narrow band is adequate for the realization of the ferromagnetic state of this polymer.

(5) By crystal orbital analysis of the cationic state, the up-spins are distributed on the carbon atoms not only in the oligothienylene unit but in part of the *m*-phenylene unit. This indicates that the *m*-phenylene unit can work as an FCB.

These findings indicate that P*m*PhTh$_4$ could be a polaronic ferromagnet polymer. Although interchain coupling might be antiferromagnetic, the spins on the chain should be ferromagnetically coupled. Further confirmation of this ferromagnetic coupling will be reported in the near future.

This work is a part of the project of the Institute for Fundamental Chemistry, supported by Japan Society for the Promotion of Science—Research for the Future Program (JSPS-RFTF96P00206). Numerical calculations were carried out at the Data Processing Centre of Kyoto University. One of the authors is grateful to Dr M. Okada in the Institute for Fundamental Chemistry for technical help in the CO calculations.

References

1 N. Mataga, *Theoret. Chim. Acta*, 1968, **10**, 372.
2 H. Fukutome, A. Takahashi and M. Ozaki, *Chem. Phys. Lett.*, 1987, **133**, 34.
3 D. A. Kaisaki, W. Chang and D. A. Dougherty, *J. Am. Chem. Soc.*, 1991, **113**, 2764.
4 See, for instance, J. Roncali, *Chem. Rev.*, 1992, **92**, 711 and references therein.
5 D. Fichou, G. Horowitz and F. Garnier, *Synth. Met.*, 1990, **39**, 125.
6 K. Waragai and S. Hotta, *Synth. Met.*, 1991, **41–43**, 519.
7 S. Hotta and K. Waragai, *J. Phys. Chem.*, 1993, **97**, 7427.
8 J. Cornil, D. Beljonne and J. L. Bredas, *J. Chem. Phys.*, 1995, **103**, 842.
9 T. Mitsuhara, S. Tanaka and K. Kaeriyama, *Makromol. Chem.*, 1988, **189**, 1755.
10 M. M. Murray, P. Kaszynski, D. A. Kaisaki, W. Chang and D. A. Dougherty, *J. Am. Chem. Soc.*, 1994, **116**, 8152.
11 T. Sato, K. Hori, K. Tanaka, M. Fujitsuka, A. Watanabe and O. Ito, submitted to *J. Phys. Chem. A*.
12 K. R. Fernando, A. J. McQuillan, B. M. Peake and J. Wells, *J. Magn. Reson.*, 1986, **68**, 551.
13 A. Terahara, H. Ohya-Nishigushi, N. Hirota and A. Oku, *J. Phys. Chem.*, 1986, **90**, 1564.
14 A. Imamura and H. Fujita, *J. Chem. Phys.*, 1974, **61**, 115.
15 K. Tanaka, T. Shichiri, M. Kobashi and T. Yamabe, *Synth. Met.*, 1988, **24**, 167.
16 Y. Furukawa, M. Akimoto and I. Harada, *Synth. Met.*, 1987, **18**, 151.
17 T. Yamamoto, K. Sanechika and A. Yamamoto, *Bull. Chem. Soc. Jpn.*, 1983, **56**, 1497.
18 J. Guay, P. Kasai, A. Diaz, R. Wu, J. M. Tour and L. H. Dao, *Chem. Mater.*, 1992, **4**, 1097.
19 J. Roncali, M. Lemaire, R. Garreau and F. Garnier, *Synth. Met.*, 1987, **18**, 139.
20 Y. Matsuura, Y. Oshima, Y. Misaki, H. Fujiwara, K. Tanaka, T. Yamabe and S. Hotta, *Synth. Met.*, 1996, **82**, 155.
21 A. O. Patil, A. J. Heeger and F. Wudl, *Chem. Rev.*, 1988, **88**, 183.
22 T.-C. Chung, J. H. Kaufman, A. J. Heeger and F. Wudl, *Phys. Rev. B*, 1984, **30**, 702.
23 K. Kaneto, S. Hayashi, S. Ura and K. Yoshino, *J. Phys. Soc. Jpn.*, 1985, **54**, 1146.
24 H. Ago, T. Kuga, T. Yamabe, K. Tanaka, A. Kunai and M. Ishikawa, *Chem. Mater.*, 1997, **9**, 1159.
25 K. Tanaka, Y. Matsuura, Y. Oshima, T. Yamabe and S. Hotta, *Synth Met.*, 1994, **66**, 295.
26 I. B. Goldberg, H. R. Crowe, P. R. Newman, A. J. Heeger and A. G. MacDiarmid, *J. Chem. Phys.*, 1979, **70**, 1132.
27 K. Fukui and K. Tanaka, *Bull. Chem. Soc. Jpn.*, 1977, **50**, 1391.
28 J. Kondo, *The Physics of Dilute Magnetic Alloys* (in Japanese), Syokabo, Tokyo, 1983.

Paper 7/06706B; *Received* 15*th September*, 1997